1.0 INTRODUCTION

Multiphase mixing in turbulent flows is a key element in many practical energy conversion, chemical mixing and pollutant dispersal problems. Numerous important technological and environmental processes could be better addressed with improvements in understanding in this area. Progress in developing understanding of this field, however, has traditionally been difficult because of the complexities involved with the turbulent flows employed to provide the mixing mechanisms.

To address this problem from a new perspective several years ago this research group initiated an ongoing investigation concerning the potential connections between organized turbulent vortex structures and the particle dispersion process. During the last 3.5 years this work has been supported primarily by the Department of Energy under grant number DE-FG06-86ER18567.

Organized vortex structures in single phase free shear flows have been studied extensively in the recent past [Ho and Huerre, 1984] because of their apparent importance in the global flow development. However, the relationship between organized vortex structures and the particle dispersion process was largely unknown. A simple physical concept which identified the Stokes number, a time scale ratio between the particle aerodynamic response time and the characteristic organized vortex motion time, as a controlling parameter for the particulate dispersion process was used to initially guide this new approach [Crowe, Gore and Troutt, 1985; Crowe, Chung and Troutt, 1989]. The Stokes number can in fact be shown to be the controlling parameter in the particle motion equation for situations where the particle material density is much greater than the local fluid density and the particle Reynolds number is small [Chung and Troutt, 1988]. To emphasize the role organized vortex motions play in the particle dispersion process this research program has focused on free shear flows such as mixing layers, jets and wakes since the organized vortex structures in these chaotic, single phase flows are probably the most clearly characterized and understood [Ho and Huerre, 1984]. Although these flows do exhibit instantaneous, three dimensional, small scale structures, their primary development is closely tied to the large scale, quasi two-dimensional structures [Browand and Troutt, 1985].

The results from these analytical, experimental and numerical research efforts concerning particle dispersion in free shear flows have yielded some extremely interesting insights into the dispersion process and its connection to the organized vortex development. These findings can be summarized as follows:

a) The qualitative and quantitative character of the particle dispersion patterns in mixing layers, jets and wakes are strongly dependent on Stokes number and can be instantaneously highly anisotropic and nonhomogeneous [Crowe, Chung and Troutt, 1989; Chung and Troutt, 1988; Tang* *et al.*, 1990a]

b) The lateral particle dispersion in both mixing layers, jets and wakes maximizes at intermediate values of Stokes number with intermediate Stokes

* See also Appendix A

numbers particles dispersing faster than the flow itself [Crowe, Chung and Troutt, 1989; Chung and Troutt, 1988; Tang *et al.*, 1990a].

c) The relative organization of the dispersion patterns in both mixing layers and wakes as quantified by the fractal correlation dimension also maximizes at intermediate values of Stokes number [Troutt, Crowe and Chung, 1990; Tang *et al.* , 1990a].

d) In mixing layers a stretching and folding operation associated with vortex structure development and pairing appears to be a dominant intermediate Stokes number particle dispersion mechanism. [Wen, 1990 & Wen *et al.*,1990]

e) In wakes where vortex pairings rarely occur, the dispersion process focuses intermediate Stokes numbers particles into extremely thin sheet-like regions near the boundaries of the vortex structures [Troutt *et al.*, 1990; Tang *et al.*, 1990a].

The previously cited results have addressed primarily flows for which the effects of the particles on the shear flow were neglected, one-way coupling. Of considerable scientific and technological interest is the more complex situation where two-way coupling effects between the particles and the flow exist. This situation has been initially addressed quite recently by our group using stability analysis and numerical simulations involving mass and momentum two-way coupling effects (Yang *et al.*, 1990 and Tang *et al.*, 1990b). This proposal addresses the two-way coupling situation involving mass and energy coupling between the flow and particles or droplets. This type of coupling is of high technological interest and has the potential for greatly affecting the resultant flows. Previous analytic and numerical studies by this group [Yang *et al.*, 1990; Tang *et al.*, 1990c] have shown that momentum coupling works strictly as a stabilizing effect and is not significant unless relatively high loadings are encountered. For these reasons this proposal will emphasis mass and energy coupling effects which have the potential to be significant even at low to moderate loading levels.

2.0 RESEARCH OBJECTIVES

The study of coupled multiphase turbulent vortex structures represents a new research thrust in the area of particle-gas turbulence interaction. Previous studies by our group have shown that the dispersion character of a dilute particle distribution in a free shear flow is strongly dependent on the organized motion of the large scale vortex structures. However, little definitive information is available on the reverse effect of particles on the properties of the turbulent structures and the accompanying particle dispersion. This is a fruitful area of research because of its potential to provide significant new information and insight concerning turbulence-particle interactions and its potential for improving the design of energy systems.

The overall objective of this research is to investigate experimentally and numerically the effects of mass and energy coupling on the development of large scale turbulent structures and particle (droplet) dispersion in multiphase mixing layers.

This objective is to be achieved by:

• Experimental studies using flow field visualization, digital image analysis and laser point sensor measurements.

• Numerical simulations using discrete vortex formulations with two-way coupling.

• Interpretations of the coordinated experimental and numerical results to gain insight concerning the effects of particles on the flow development and mixing process.

3.0 BACKGROUND

3.1 Previous Findings

Traditionally the particle dispersion process has been modeled as a Fickian diffusion process in conjunction with time-averaged dependent variables such as velocity and particle concentration. This model may be adequate for isotropic flow fields, however, the majority of particle mixing and dispersion problems involve shear-driven turbulent flows in which the mean velocity gradient produces anisotropic large scale turbulent structures. These organized vortex structures have the potential to be instrumental in the mechanics of the particle dispersion process. In fact, there is now considerable experimental and numerical evidence available demonstrating that large-scale structures promote unexpectedly large and orderly particle dispersion effects which can not be explained by the conventional dispersion theories [Crowe, Chung and Troutt, 1989]. Also studies using direct numerical simulation [Squires and Eaton, 1989] have shown that even small scale organized vortices play a key role in dispersing particles.

For the past five years, a physical model based on the mechanics of the large-scale vortices and their interactions with particles has been developed by our group at Washington State University. This model has been verified by numerical simulations and experimental results. A detailed description of the model and its development are given in a recent review article by the authors [Crowe, Chung and Troutt, 1989]. The central idea of this model is that the particle dispersion process in turbulent shear flows is dominated by the ratio of the particle aerodynamic response time to the characteristic time associated with the organized vortex structures. This ratio is usually referred to as the Stokes number. Particles with the Stokes number much less unity will follow closely the fluid pathlines and disperse at the rate of the fluid particles. On the other hand, particles with Stokes numbers much larger than unity, will be little affected by the flow field and thus will disperse much more slowly than the fluid particles. For a Stokes number on the order of unity, however, one might expect the particles to disperse at rates greater than that of the fluid particles because the circulatory flow patterns of the vortex structures create a centrifuging effect which causes the particles to be flung out of the cores of the vortex structures. This physical model is illustrated in Fig. 1.

Verification of this physical model was initially pursued using analytical and numerical techniques and the assumption of one-way coupling, that is, the particles were assumed to have no effect on the flow field. An initial simulation using Stuart's distributed vortex solution for a time developing free shear layer was given in Crowe, Gore and Troutt [1985]. Later efforts for simulating particle dispersion in plane free shear layers employed discrete vortex techniques [Chien and Chung, 1988 and Chung and Troutt, 1988] and pseudo spectral approaches [Gore *et al.*, 1989]. All of these simulations strongly supported the physical concept that enhanced particle dispersion would occur near a Stokes

number of unity. Predicted instantaneous particle dispersion patterns from Wen *et al.* [1990] for particles in a free shear layer at three Stokes numbers are shown in Fig. 2. In this simulation the flow is from left to right with the high speed stream on the top. The predicted patterns strongly support the concept of enhanced dispersion at intermediate Stokes numbers. The level of enhanced dispersion can be easily quantified by employing a dispersion function [Chung and Troutt, 1988]. The computations show that enhancements of over 150% can be realized over that of a fluid particle in a mixing layer.

Experimental studies concerning the dispersion of particles by large scale structures have also recently been carried out in our laboratory. These studies have focused primarily on the plane mixing layer and wake flows and have involved instantaneous flow and particle visualization experiments coupled with time-averaged laser velocimetry techniques. Instantaneous results from the mixing layer visualization studies [Kamalu *et al.* 1988] are shown in Figs. 3 and 4. A visualization of the carrier air flow field using the smoke wire technique (with diffuse flash lighting) is shown in figure 3a. The smoke consists of particles approximately 1μm in diameter for which the Stokes number is very small ($St << 1$) and the smoke tends to fill the vortex cores. The dispersion pattern of 40 μm diameter glass particles obtained using diffuse light photography is shown in figure 3b. The Stokes number is of order unity in this figure and the near absence of particles in the large scale vortex cores is obvious. Computations involving particle concentration levels from these experiments also support the concept of enhancement in dispersion levels at intermediate Stokes numbers [Kamalu, 1989]

Further evidence of the importance of Stokes number is illustrated in figure 4. These pictures are the result of laser-sheet photography of the dispersion patterns for 10 and 40 μm particles. The Stokes number for the 40-micron particles is near unity and one notes the tendency for the particles to be centrifuged to the peripheries of the vortices. The particle dispersion patterns are strikingly similar to the simulation patterns shown previously. The nonhomogeneous and anisotropic nature of the particle dispersion process is apparent in these figures.

Experimental laser velocimetry results for the gas flow field and the 40 μm diameter particles also support the trends predicted by the model. The data for the cross stream velocity component of the air and particles show that the air flow is directed towards the center of the mixing layer while the particle velocities are directed away from the mixing layer. These results again indicate that intermediate particle dispersion may be controlled by the large scale vortices. A description of these experimental efforts is given in Wen *et al.* [1990]. Moreover, a more detailed mechanism for explaining intermediate particle dispersion involving a stretching and folding process has been recently suggested by Wen *et al.* [1990].

In addition recent experimental and numerical efforts have been directed at non-coupled particle dispersion in plane wakes. These results have shown that the particle dispersion process in wakes is even more highly organized than the plane mixing results for intermediate Stokes number particles. In addition, extremely high particle dispersion rates of over 600% relative to fluid element rates have been computed from these results. Numerical simulations of the plane wake results at various Stokes numbers are shown in Fig. 5. A quantitative evaluation of the wake flow dispersion obtained using the mixing function is shown in Fig. 6. The mixing function is defined as $D_f = \frac{1}{N}\sum_0^N (y - y_i)^2$ where N is the total number of particles, y_i is the initial lateral position of the particle and y is

the lateral position at a later time. A detailed description of the plane wake results are included in Appendix A.

Recent work at WSU has also been directed toward extending the discrete vortex method to include multiphase coupling effects. The presence of particles in the carrier fluid represents a potential source (or sink) of mass, momentum or energy. The effort to this point has been directed towards momentum coupling resulting from the aerodynamic drag on the particles.

The results of preliminary numerical work on the effect of momentum coupling on the shear layer development have been obtained are provided by Tang *et al.* [1989] which is included in Appendix B. This work addressed the temporal development of multiphase flow in a cell which models flow development in a mixing layer associated with a reference frame moving at the average velocity of the flow. Temporal plots of the vortex and particulate fields illustrate the retardation of vortex formation due to momentum coupling effects with the particles. More quantitative results are obtained by calculating the increase in momentum thickness of the shear layer with time which clearly show the slower development of the multiphase shear layer. Calculations are continuing to establish the relative effects of Stokes number, particle concentration and initial velocity ratio on the shear layer growth.

The numerical scheme for coupling effects has been extended [Tang *et al.*, 1990c] to also include mass coupling effects; specifically the effect of mass addition due to droplet evaporation. These studies have shown that mass coupling tends to impede the development of the large scale structures. The lateral motion of the droplets is therefore caused by both the expansion of the flow field resulting from mass addition and the centrifuging of the droplets by the large scale structures.

3.2 Analytic Procedure for Implementing Coupling Effects

One objective of the present proposal is to extend the existing modeling effort to include compressibility effects and energy coupling. This development can be viewed as a logical precursor to including heat release due to chemical reaction and the analysis of multiphase combustion in large scale turbulent structures. The technique is an extension of that reported by Ghoniem *et al.* [1987] for compressible reacting flows using the discrete vortex method together with transport elements.

The velocity field in the model is decomposed into three parts; the field corresponding to the basic potential flow, the velocity induced by the vortices in the field and the field caused by the mass release from the droplets. Including compressibility effects leads to a change in the strength of the mass sources and also affects the circulation of the discrete vortices.

The continuity equation for the gas phase of a droplet-laden flow with void fraction near unity is

$$\nabla \cdot \vec{u} = \frac{S_m}{\rho} - \frac{1}{\rho}\frac{D\rho}{Dt}$$

where S_m is the mass source per unit volume due to droplet evaporation or condensation. For low Mach numbers, one can make the assumption that the pressure level is constant

so, for an ideal gas, the continuity equation becomes

$$\nabla \cdot \vec{u} = \frac{S_m}{\rho} + \frac{1}{T}\frac{DT}{Dt}$$

where T is the local temperature. The right side of this equation represents the strength of the mass source term associated with each droplet. The last term represents the local expansion of the flow due to local heating or cooling.

The momentum equation for the the gas phase of a dispersed phase flow at high Reynolds number and void fraction near unity is

$$\frac{D\vec{u}}{Dt} = -\frac{1}{\rho}\nabla p + \frac{1}{\rho}[(\frac{f\rho_d'}{\tau_A} + S_m)(\vec{v} - \vec{u})]$$

where f is the ratio of the drag coefficient to Stokes drag, τ_A is the aerodynamic response time of the droplet, ρ_d' is the bulk density of the droplets and $\vec{v}$ is the velocity of the droplet phase. It is assumed that the viscosity is important only in the the immediate neighborhood of the droplets. The last term in the above equation is due to momentum coupling and is calculated from the droplet trajectories. For convenience this term is simplified to $\vec{C}$ so the equation can be rewritten more simply as

$$\frac{D\vec{u}}{Dt} = -\frac{1}{\rho}\nabla p + \frac{1}{\rho}\vec{C}$$

Taking the curl of the momentum equation and limiting the solution to two-dimensional flows yields

$$\frac{D\omega}{Dt} - \frac{\omega}{\rho}\frac{D\rho}{Dt} = \frac{1}{\rho}\nabla\rho \times (\frac{\nabla p}{\rho} - \frac{\vec{C}}{\rho}) + \frac{1}{\rho}\nabla \times \vec{C}$$

In the discrete vortex approach the flow field is subdivided into material elements with circulation Γ. Since the mass of a material element is constant, the derivative of the density can be related to the area change of the element (in planar flow) by

$$\frac{1}{\rho}\frac{D\rho}{Dt} = -\frac{1}{A}\frac{DA}{Dt}$$

Substituting this expression into the vorticity equation and using the momentum equation leads to

$$\frac{D(\omega A)}{Dt} = -\frac{A}{\rho}\nabla\rho \times \frac{D\vec{u}}{Dt} + \frac{A}{\rho}\nabla \times \vec{C}$$

The product of the vorticity and the area is the circulation of the vortex. Using the low Mach number assumption by which the density variation is associated with the temperature change only, the expression for the change in circulation of each discrete vortex is

$$\frac{D\Gamma}{Dt} = \frac{(A\rho)_o}{\rho}\frac{\nabla T}{T} \times \frac{D\vec{u}}{Dt} + \frac{A}{\rho}\nabla \times \vec{C}$$

where $(A\rho)_o$ is the initial cross-sectional area times the density of the material element. This product, which is proportional to the mass of the element, remains constant. The first term on the right side is the effect of density change on the vortex strength and the

last term is that due to multiphase coupling. The coupling term is to be evaluated in the same manner used previously for the mass and momentum coupling. That is, the droplet trajectories provide locations and properties of the droplets in the field. The properties are area-averaged to nodal points on a grid and the coupling term is evaluated and distributed to each vortex in the cell.

In order to calculate the change in circulation, the temperature field (and density) is needed. This is obtained from the transport-element method introduced by Ghoniem *et al.* [1987]. The energy equation for the gaseous phase of a high Reynolds number dispersed phase flow is

$$\frac{DT}{Dt} = \frac{\rho_d'}{\rho}\frac{1}{\tau_T}(T_d - T)$$

where τ_T is the thermal response time of the droplet and T_d is the droplet temperature. For convenience, the thermal coupling term is simplified to $\dot{Q}_d$ so the energy equation becomes

$$\frac{DT}{Dt} = \frac{\dot{Q}_d}{\rho}$$

In the transport element method, the change in the gradient of the temperature of a fluid element is obtained. For convenience, the transport element is usually the vortex element. Taking the gradient of the energy equation results in

$$\frac{D(\nabla T)}{Dt} = \nabla T \cdot \nabla \vec{u} - \nabla T \times \omega + \nabla(\frac{\dot{Q}_d}{\rho})$$

The first two terms represent the strain and rotation of the material element by the local strain field and vorticity. The last term is the multiphase coupling term which will be evaluated from the trajectories and temperatures of the droplets and by distributing the source term to each transport element in the cell.

Having the strength and location of the transport elements one can calculate the temperature (and density) field by taking the gradient of the temperature gradient to yield Poisson's equation ($\nabla^2 T = f(x, y)$). The solution of Poisson's equation gives the temperature field. It is also possible to include a finite diffusivity in the energy equation by letting the core radius grow with time [Ghoniem *et al.*, 1987].

The mass fraction of the droplet vapor in the gas flow can also be obtained by using transport elements with the gradient of the vapor mass fraction. In this case the source term equivalent to $\dot{Q}_d$ in the energy equation is the mass of vapor added per unit volume due to evaporation; that is, S_m, which the mass coupling term appearing in the gas- phase continuity equation.

The droplet properties will be obtained by integrating the droplet mass, motion and energy equations along trajectories in the flow field. This is called the Lagrangian approach. The droplet continuity equation is

$$\frac{dm}{dt} = -Sh\rho D_v d(x_d - x)$$

where Sh is the Sherwood number, D_v is diffusion coefficient, x_d is the mass fraction of droplet vapor at the droplet surface (a function of droplet temperature) and x is the mass fraction of droplet vapor in the free stream.

The droplet motion equation is

$$\frac{d\vec{v}}{dt} = \frac{f}{\tau_A}(\vec{u} - \vec{v}) + \vec{g}$$

where it has been assumed that the vapor exits uniformly from the droplet surface.

The droplet energy equation is

$$\frac{dT_d}{dt} = \frac{(T - T_d)}{\tau_T} + \frac{h_L}{mc_p}\frac{dm}{dt}$$

where h_L is the latent heat of fusion and c_p is the specific heat of the droplet liquid.

These equations complete the set required to develop a completely coupled numerical model for the multiphase shear flows and wakes.

4.0 RESEARCH METHODOLOGY

4.1 Overview

The objective of the proposed research program is to determine the effects of two-way coupling on the development of multiphase free shear flows. The proposed research will be conducted through a closely coordinated experimental and numerical program building on the expertise and experience gained through our previous research efforts in multiphase shear flows.

The basic flow configuration will involve two-stream free shear flows produced downstream of a parallel surface splitter plate. The thickness of the splitter plate will be variable such that a range of δ/d flow parameters can be investigated.

$$\delta/d << 1, \qquad \delta/d \sim O(1), \qquad \delta/d >> 1$$

Here δ is the plate trailing edge boundary layer thickness and d is the plate trailing edge thickness. A schematic showing the basic flow arrangement is presented in Fig. 7. The variation of δ/d significantly affects the initial development of plane wake flows [Wygnanski *et al.*, 1985 and Hanle, 1988]and therefore their potential particle dispersion characteristics. Both experimental plane wakes and mixing layers can be generated from this general experimental arrangement by adjustment of the free stream velocities, U_H and U_L, (Mixing layers are a practical result when U_H/U_L is significantly greater than unity.) This research will investigate the coupling effects in both wakes and mixing layers since both flows offer interesting and contrasting phenomena (see Appendix A for details). Single phase plane free shear flows have been extensively investigated in the recent past [Ho and Huerre, 1984]and have been established as being the optimum flows for studying large scale organized vortex processes. Moreover, our ongoing research program in non-coupled particle dispersion has extensively concentrated on these two types of planar free shear flows.

The emphasis in this program will primarily concern two-way coupling through mass and energy exchange between the droplets (water droplets) and the dispersing medium (heated air) since recent numerical results [Tang *et al.*, 1990b] have indicated that momentum coupling between heavy particles and the gas flow medium is relatively inefficient, compared to mass coupling, at low to moderate loading concentration. Although no numerical or experimental results are presently available we expect energy

coupling to play a role at least as significant as mass coupling in affecting the shear flow dispersion process. Moreover, two-way mass and energy coupling dispersion processes represent a technologically important area since many energy conversion systems involving turbulent processes have operate at low to moderate loading levels which indicates that momentum coupling is probably of secondary importance.

This research program will include two closely matched components: (1) experimental and (2) numerical. The experimental component will involve multiphase flow visualization with digital image analysis for determining quantitative results and point sensor laser Doppler anemometery with a phase Doppler extension. The results of these experimental measurements will provide both local and global information concerning multiphase droplet velocities, concentration levels and sizes as well as gas velocity information.

The numerical research component will extend numerical work already in progress [Tang *et al.*, 1990a,b] concerning momentum and mass coupled effects between the gas and particle phases. The proposed numerical work will concentrate extensively on the mass and energy coupling effects associated with vaporizing droplets in a gas flow. These effects will be included into discrete vortex simulations by adding mass and energy sources into the modelling equations and allowing for compressibility effects in the governing equations.

The specific quantities to be measured in the proposed experimental and numerical programs are now listed.

	Experimental Component	Numerical Component
Point Flow Velocity (instantaneous and time average)	X	X
Droplet Velocities (instantaneous and time average)	X	X
Droplet Sizes (instantaneous and time average)	X	X
Droplet Dispersion Characteristics (including standard statistical dispersion functions, particle concentration contours, and chaotic dimension analysis.)	X	X

Details on the experimental and numerical programs can be found in Sections 4.3 and 4.4 respectively.

4.2 Facility Design

A new facility will be expressly designed and constructed for this program with institutional support. The basic design will be similar to the successful cold flow facility used for our previous work on particle dispersion in shear flows. The new facility will be approximately the same size with a test section 0.5 m high, 1 m wide and 2 m long. It will be fabricated using thermally stable insulating materials to facilitate operation at temperatures between 100 and 200°C. Electrical power requirements for the heating section can be easily satisfied by our existing laboratory capabilities. A schematic diagram of the new facility is shown in figure 8. The flow will be supplied by a radial fan and the

of the new facility is shown in figure 8. The flow will be supplied by a radial fan and the flow rate will be controlled by a valve at the inlet. The air will enter a heating section where it will be heated by electric coils to a temperature between 100° and 200°C. A fifth order contour contraction section with contraction ratio of 9 to 1 and a flow conditioning section will be used to achieve low free stream turbulence intensities $O(0.1\ \%)$ and uniform velocity profiles with mean flow uniformity within $\pm 0.1\%$ in the test section.

Various δ/d geometry where δ is the boundary layer thickness ($0.1 < \frac{\delta}{d} < 10$) wake flows will be generated by interchanging sections at the end of the splitter plate (and employing boundary layer suction techniques). In addition the tunnel will be mounted vertically to eliminate any potential for significant gravitational effects with respect to transporting larger droplets laterally across the flow at low free stream velocities. The gravitational drift velocity will be maintained at small values relative to the convective flow velocity.

The droplets will be supplied by pressure atomizers which can be mounted in the downstream face of the bluff body or at locations above (or below) the splitter plate. These pressure atomizers will used filtered water at room temperature and will produce droplets in a full cone pattern with a Sauter mean diameter of the order of 100 microns. There will be an array of atomizers to insure homogeneous injection patterns. The pressure atomizer avoids the complexity of atomizing air being injected into the flow field. The wide variety of spray patterns possible (square, flat spray, etc.) will also allow tailoring the injection configuration to achieve two-dimensional patterns for simplifying the interpretations of the dispersion phenomena.

The range of other important non-dimensional parameters to be covered in this research are provided below. To investigate coupling effects on droplet focusing processes in the wake, the Stokes number range of the droplets must be extend above and below unity. The aerodynamic response time of a 100 micron water droplet in air at 100° C is approximate 25 ms. With typical values of flow velocity, 5 m/s, with a trailing edge width, 2 cm, a droplet Stokes number of unity results. Higher and lower Stokes numbers can be obtained with higher/lower velocities and larger/smaller plate widths. The practical Stokes number range will be 0.1 to 10. Reynolds numbers of the air flow on the order of 10^3 to 10^5 will be obtainable with the proposed experimental facility.

The potential effect of thermal coupling on the air flow can be assessed by the ratio of the gas-droplet heat transfer rate per unit volume to the enthalpy flux of the air. This ratio is given by

$$\frac{\dot{Q}_d}{\dot{m} h_g} = \frac{\rho_p'}{\rho} \frac{L}{U \tau_T} \frac{\Delta T}{T_g}$$

where ρ_d' is the bulk density of the droplets, L is a characteristic dimension of the flow field (width of trailing edge for the wake) and τ_T is the thermal response time of a droplet. The ratio of the droplet bulk density to the gas density is proportional to the droplet /air mass flow ratio. A loading of two can be is easily achieved with 5 cm spacing between atomizers. The thermal response time of a water droplet in air is the same order of magnitude as the aerodynamic response time. For the typical flow situation discussed previously, the ratio of gas-droplet heat transfer to the enthalpy flux of the air for 100 micron droplets in air at 100° C flowing over a 2 cm edge at 5 m/s is approximately 0.6. Thus there would be significant potential for thermal coupling effects. The effects would even be more intensified in the regions of particle focusing in the wake.

The experimental conditions to be covered in proposed research are listed in the following table.

Parameter	Symbol	Parametric range
Boundary layer thickness to plate thickness ratio	δ/d (wake)	0.1 - 10
	δ/d (mixing layer)	>10
Reynolds number	Re	10^3 - 10^5
Stokes number	St	0.1 - 10
Heat Transfer Rate Ratio	$\dot{Q}_d/\dot{m}h_{fg}$	0.0 - 1.0

4.3 Experimental Techniques

Two types of measurements will be carried out in the facility; flow field and particle visualization for determining local and global information concerning the droplet flow patterns and point sensor measurements for establishing local droplet and flow properties.

Experiments in visualization will be carried out using high speed photographic techniques synchronized with illumination by a laser-light sheet. Two excellent illumination sources for the light sheet are available; a 20 watt pulsed copper-vapor laser and a 5 watt argon-ion continuous wave laser. The optical components for this system are already available in our laboratory. The laser light sheet will be used to illuminate both instantaneous flow and particle patterns. The flow and particle dispersion patterns will be visualized both individually and conjointly. The gas flow field will be visualized using very fine particles (very small Stokes number) to trace the flow fluctuations. The particles will be injected into the flow upstream of shear flow origin. Simultaneously, droplets with a narrow size distribution will be introduced from the injector to enable direct comparisons between the flow and particle dispersion patterns.

Quantitative information can be obtained from the visualization results with the use of image analysis techniques [Kamalu, *et al.*, 1989]. Two image analysis systems are presently available for extracting this information: a departmental system (Imaging Technologies System with 512 x 512 pixel resolution) and a university supported system (Eikonix System with 4096 x 5200 pixel resolution). If it is assumed that the reflected light intensities are related to droplet concentration levels then the acquired photographs can be evaluated to give instantaneous droplet dispersion levels throughout the flow. This assumption concerning reflected light intensities and their relationship to droplet concentration levels is reasonable even at relatively high droplet loadings [Van de Hulst, 1957]. Droplet concentration levels can also be determined directly by counting individual droplets with digital analysis techniques. A technique is now being developed in our current work involving non-coupled solid particle dispersion. Time-average information can also be obtained from the visualization experiments by employing multiple film exposure techniques. This type of time average information can be compared directly with the information obtainable from laser velocimetry methods (and light reflection concentration levels) discussed below.

Instantaneous droplet motion will also be tracked with a high speed motion picture camera capable of 10,000 frames per second (NAC Model E-10) using laser sheet lighting from the 20-watt pulsed Copper-vapor laser by synchronizing the camera framing rate with the laser pulses. This laser provides sufficient light intensity to freeze the particle position with time. Pulse duration is typically 20 μs with continuous succession pulse rates up to 10,000 Hz. These data will be useful in indicating the developing motion of the droplet clouds and providing a qualitative indication of droplet concentration.

Successive frames of the high speed motion film can be digitized to provide information not only concerning droplet positions but also droplet velocities. The droplet velocities can be computed directly by the approximation $\vec{v}_p \sim \frac{\Delta \vec{r}_p}{\Delta t}$ where $\Delta \vec{r}_p$ is the change in droplet position and Δt is the time between frames. These quantities can be computed efficiently using digital software developed for particle image velocimetry techniques [Kasagi and Nishino, 1990]. Digital software procedures for accomplishing these calculations are presently under development in our laboratory and are being employed currently to measure particle velocities in both water and air flow facilities. Potentially these techniques can also be employed to measure instantaneous fluid velocities if the particles have time responses small enough to keep up with the flow fluctuations. Professor Ramaprian, a departmental colleague, has used techniques of this type to recently measure wake velocity fields in a water flow with good success [Ramaprian (1990)]. These techniques can also be applied to the air flow provided air velocities are kept at levels such that particle tracer Stokes numbers are small. For the proposed experimental arrangement this requirement can be met with particles below approximately 10 μm in diameter.

Droplet size measurements will be obtained using a Particle Dynamics Analyzer which operates on the phase-Doppler principle for simultaneously obtaining particle size and velocity. The velocity of the droplet is obtained from the frequency of the reflected coherent light while the droplet size is reduced from the phase difference of the reflected light as obtained from two photo detectors placed at different angles from the scattering droplet. The resulting electrical signal received from the two photo detectors can be cross-correlated to determine the relative phase difference between the two signals. This phase difference can then be analyzed using Mie scattering theory based on Maxwell's equations to accurately determine the diameter of homogeneous spherical droplets for sizes between 1.0 and 100μm. [Saffman, 1987]. This system can be obtained by modest extension of our departmental three-dimensional laser-Doppler system. This equipment extension is cost shared at 50% by Washington State University as indicated in the proposed budget.

Droplet concentration levels can also be measured by employing laser velocimetry interdata validation times. This type of droplet concentration measurement technique has been previously employed by Fleckhaus *et al.* [1987] and Wen *et al.* [1990] to successfully measure time averaged particle concentration levels.

The experimental measurements and techniques to be used to make the measurements are listed in the following table.

Measurement	Experimental Technique
Flow velocity	Laser Doppler Anemometry

Droplet Velocity (2 and 3 dimensions)	Laser-Doppler Anemometer Particle Image Velocimetry
Droplet Concentration Distribution	Interdata time (LDA) Light reflection intensity Direct droplet counting
Droplet Size	Laser phase Doppler Anemometry

4.4 Numerical Techniques

Numerical calculations will be carried out for flow conditions and droplet properties corresponding to the experimental conditions. Specifically the flow velocity and temperature together with the liquid flow rate, droplet size and velocity will be needed to initiate the calculations. The flow diagram for carrying out the numerical simulation in shown in Fig. 9. The numerical approach will use a time-splitting scheme to circumvent iterations for incorporating coupling effects. At the beginning of each new time step, the droplets and vortices are moved to new locations corresponding to a half time step. The multiphase coupling terms and the change in circulation due to compressibility effects are evaluated at this time level. The circulation of the vortices are then updated to include the coupling effects. The temperature and density of the field are also updated. A new velocity field is calculated and the vortices and droplets are moved over the complete time step corresponding to the conditions evaluated at the intermediate time level. The procedure continues until the time limit is reached. With each time step, new droplets and vortices are added to the field while others leave the field and are excluded from the calculations.

The numerical results will be used to complement the experimental measurements of droplet concentrations, local gas and droplet velocities and droplet size. Specific quantities, such as fractal correlation dimension, will be calculated from the numerical predictions and compared with data obtained from experimental measurements. Sensitivity calculations will also be performed to assess the importance of droplet loading on the development of the large scale structures. The numerical results will also be used to yield the droplet dispersion rate so the multiphase coupling effects on dispersion can be evaluated.

5.0 FACILITIES

5.1 Experimental Equipment and Facilities

The proposed experimental study will be carried out in our newly remodeled thermal-fluids laboratory building which has approximately 10,000 sq. ft. available for experimental research. Excellent air, power and water supplies are available for carrying out the proposed experiments.

Major applicable equipment items include;
A State-of-the art three-dimensional Dantec fiber optics laser velocimeter system and two Masscomp, MC500 and MC5600 super microcomputers for data acquisition and analysis. The Masscomp computers are connected through a ethernet for fast transfer of data and

program files. The MC5600 has a 100 megabyte hard disk drive and $\frac{1}{2}$ inch tape drive for archiving the acquired data. Both of these computers are capable of digitizing up to 16 channels simultaneously with overall sampling rates of up to 1 MHz.

Other major equipment items for employment in this research include:

- Imaging Technologies SDP 151 Processing System for image acquisition and analysis which is also ethernetted to the Mass Comp computers.
- NAC high speed 16mm camera with 10,000 frames/sec capability.
- Nikon F-3 35mm camera and a Graphflex 6x4 format view camera are also available for acquiring still photographs of the flow and particle phenomena.
- Five watt continuous light Argon-Ion laser is presently available for laser sheet illumination.
- Metalaser Technology 20 watt copper vapor pulse laser.

We have also recently designed and purchased optical systems for establishing an extremely well-focused laser light sheet with either laser. We are presently undertaking experimental measurements with this laser light sheet arrangement in our on-going mixing layer and wake flow particle dispersion research.

In addition to these major equipment items, minor equipment including 16 hot-wire anemometry channels, analog filters and oscilloscopes are readily available to support the proposed research. We now consider this laboratory to be one of the best equipped laboratories in the United States for the type of research proposed here.

5.2 Computational Facilities

Direct numerical simulations of particle dispersion in turbulent wake flows by discrete vortex methods require extensive computing power. The available computing resources are listed as follows:

- IBM 3090 at Washington State University. This near-supercomputer is a large main-frame facility. Free computing time has been provided by the University. All the particle dispersion simulations performed at WSU were done on the IBM 3090.
- CRAY-XMP at Battelle Pacific Northwest Laboratories. An agreement has been worked out recently between WSU and Battelle such that WSU researchers will be able to access the CRAY-XMP through a direct line.
- CNSF - Cornell National Supercomputer Facility. WSU and CNSF have made an agreement that allows WSU to apply for substantial amount of computing time from their supercomputing facilities.
- MASSCOMP 5600 super-microcomputer which was purchased through a recent Department of Defense instrumentation grant. Its computational power is approximately one-fifth of the IBM 3090 computer. A significant amount of initial computer program development work can be carried out on this computer.

6.0 PROGRAM PLAN

The program will consist of a coordinated experimental and numerical effort. The specific tasks are outlined below and a proposed schedule for completing these tasks is provided in Fig. 8.

Task E1 Design and Fabricate Overall Test Facility

Task E2 Facility Flow Qualification Tests

Task E3 Droplet Injection Qualification Tests

Task E4 Initial Flow and Droplet Visualization Experiments

Task E5 Initial Flow and Droplet Point Sensor Experiments

Task E6 Final Flow and Droplet Experiments Involving Visualization and Sensor Measurements Emphasizing Coupled Dynamics

Numerical Tasks

Task N1 Develop Numerical Model for Multiphase Mass and Energy Coupling

Task N2 Apply Numerical Coupling Model to Multiphase Shear Flow Test Case

Task N3 Apply Numerical Coupling Model for Extensive Runs to simulate Experimental Conditions

Task N4 Apply Numerical Coupling Model Over a Broad Range of Non-Dimensional Parameters to Identify Important Experimental Tasks and Numerical Trends

Task EN1 Closely Examine and Compare Experimental and Numerical Results for Confirmation of Findings.

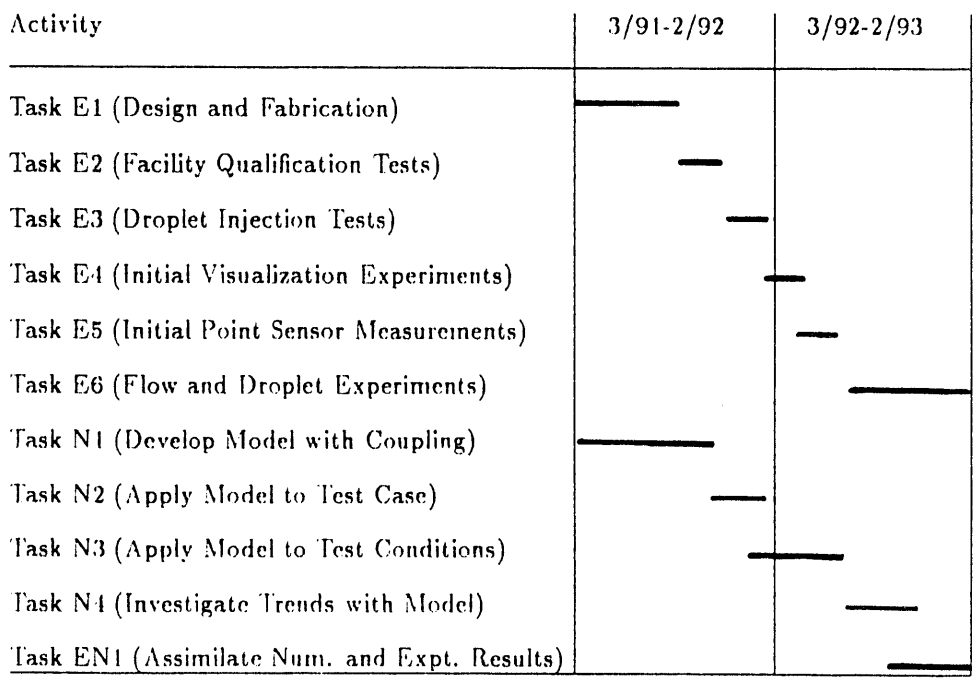

7.0 PERSONNEL

Professor T.R. Troutt will supervise and coordinate all phases of the project. He was the Principal Investigator for our previous DOE Grant No. DE-FG06-86ER13567 on particle dispersion in plane mixing layers. His experience and knowledge in this area will be effective in the administration and direction of the project. Dr. Troutt has had extensive experience over the past 15 years with experimental measurements in jets, wakes and separated flows, in addition to his recent work in the turbulent particle dispersion

area. He has also had considerable recent experience in high speed photography and digital image analysis which will significantly support the proposed project. He has also been involved recently with numerical simulations of particle-laden non-stationary flows with Professor J.N. Chung and Professor C.T. Crowe.

Professor Crowe will serve as a research collaborator for the proposed study with special emphasis on particle-flow field interactions. Professor Crowe has been working in the general area of two-phase flows for over 25 years. He has written many articles and review papers and book chapters in the general area of dispersed two-phase flows. His particle-in-cell algorithm is used extensively in industry and academia alike to model particle-fluid interaction. Professor Crowe will assist with both the experimental activities and the numerical simulation. Professor Chung will also be available in a advisory capacity to supervise activities in numerical simulations.

Half time appointments for two PhD students have also been included in the budget. One student will emphasize the experimental effort while the other will be primarily involved with the numerical simulation. Both students will have exposure to experimental and numerical work.

The resumes of the principal investigator, T.R. Troutt, and the research collaborator are provided in the Appendix.

reprint removed, ds

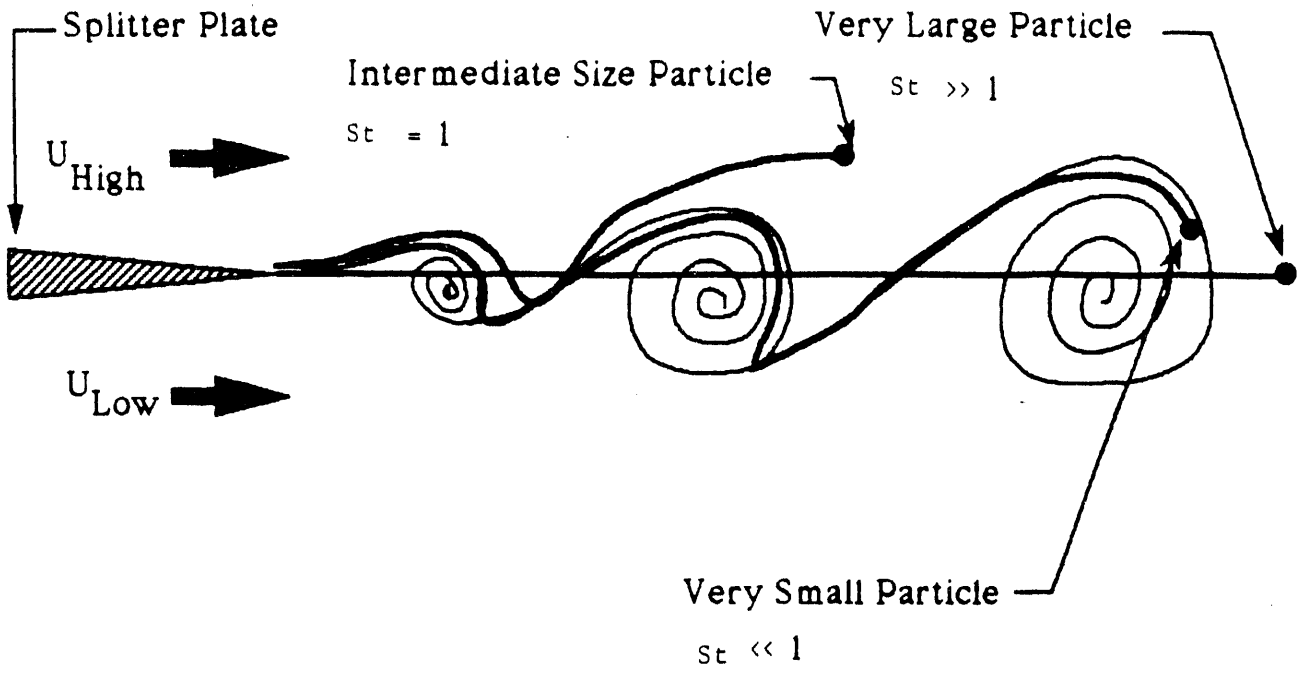

Figure 1: Schematic of Simplified Dispersion Process Model for Various Stokes Number Particles

A)

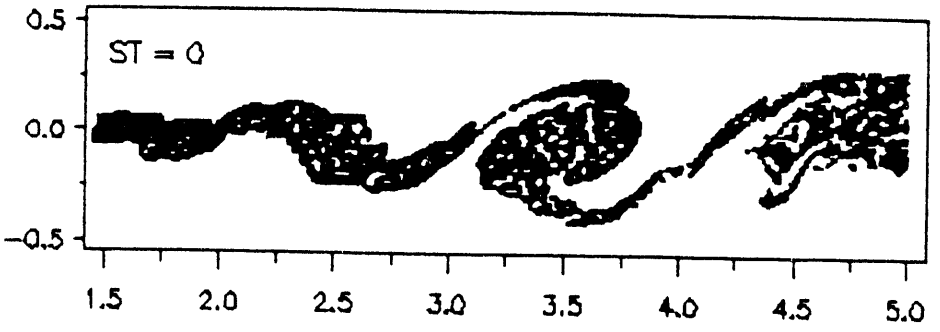

St=0 Particles

B)

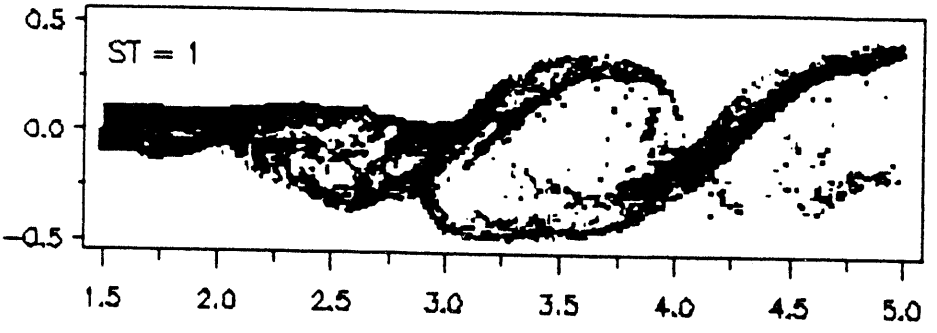

St=1 Particles

C)

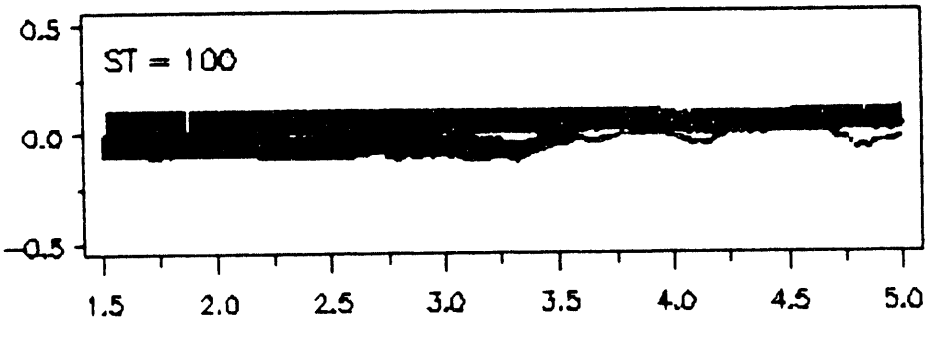

St=100 Particles

Figure 2: Numerical Simulation of Instantaneous Particle Dispersion Patterns in mixing Layer

A) Smoke Streaklines St~σ (10^{-3})

B) 40 Micron Particles ST~σ (1)

Figure 3: Experimental Visualization of Mixing Layer Flow and Particles

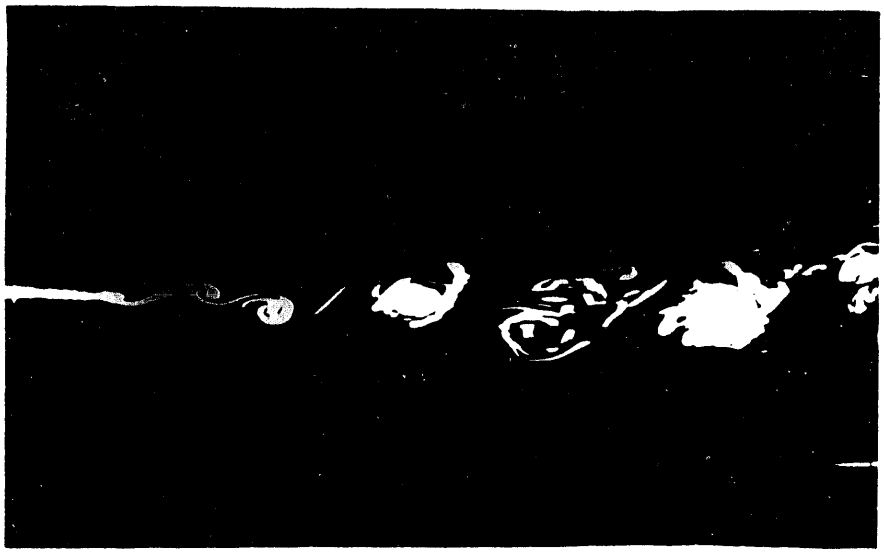

A) St~$\mathcal{O}$ (.01) Particles

B) St~$\mathcal{O}$ (1.0) Particles

Figure 4: Experimental Flow Visualization of M Layer Dispersion employing Laser Sheet Illumination

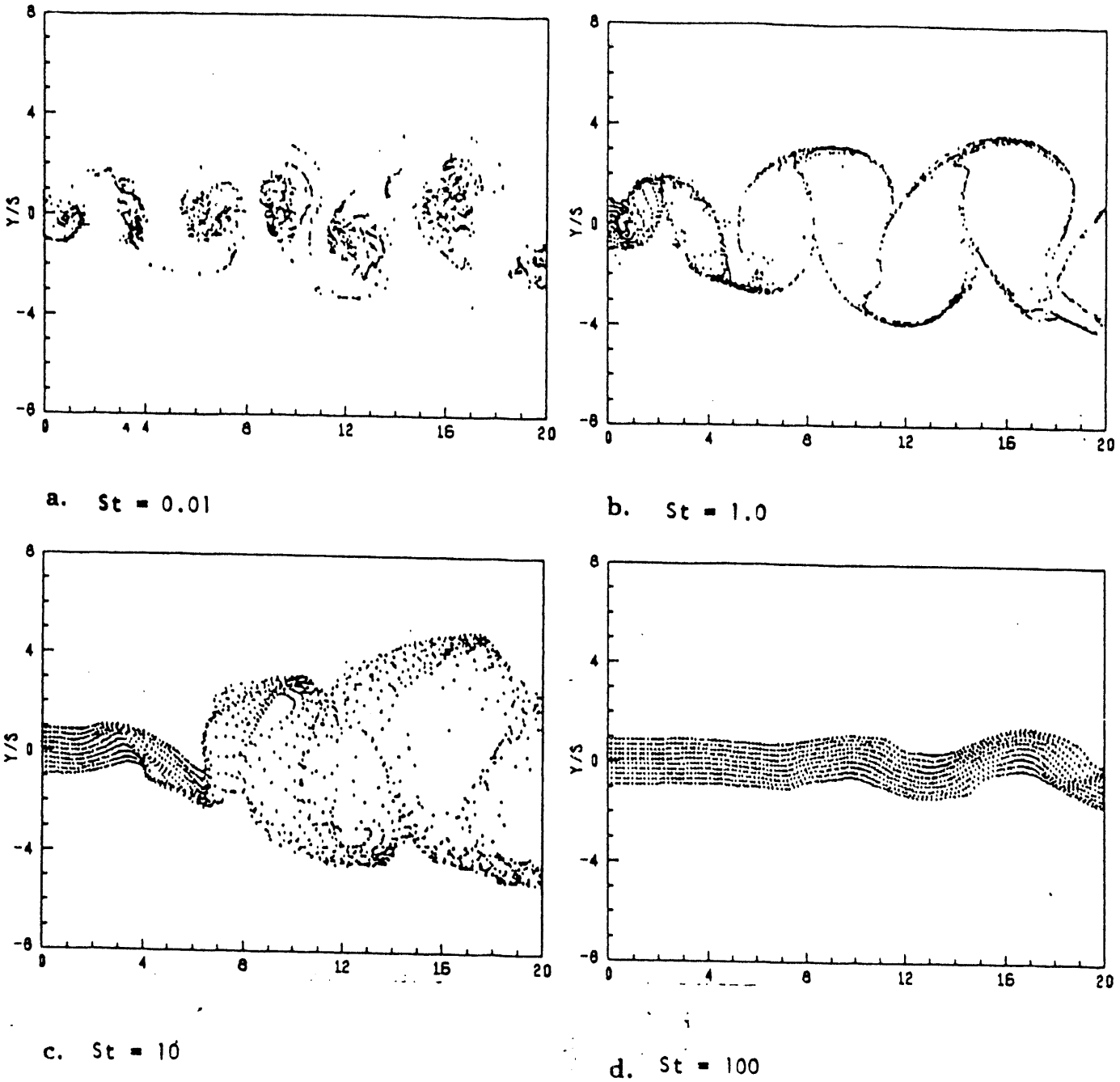

Figure 5: Numerical Simulation of Instantaneous Particle Dispersion Patterns in Plane Wake

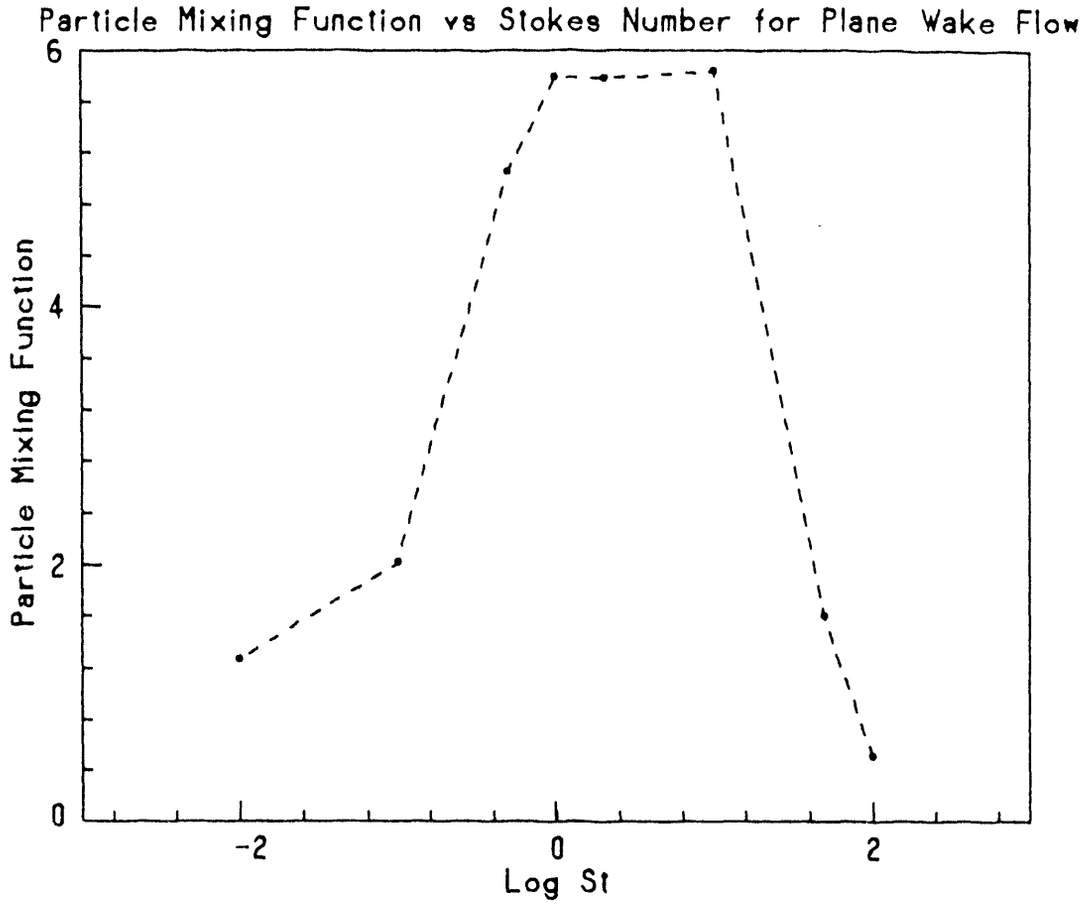

Figure 6: Normalized Particle Mixing Function from Wake Flow Simulations

END

DATE FILMED

4/5/94